

Article

Modelling Dover Harbour Using the LABSWE

Andrew Cunningham ^{1,†,‡}, Jian Zhou ^{1,‡} and Jon Shiach ^{2,*}

School of Computing, Mathematics and Digital Technology, Manchester Metropolitan University ¹
12017213@stu.mmu.ac.uk

* Correspondence: 12017213@stu.mmu.ac.uk

Version April 9, 2020 submitted to Journal Not Specified

Abstract: Dover Harbour requires significant dredging of sediment around the harbour entrances annually for its normal operation. With the recent revival of the western harbour a significant portion of this sediment has been resourced to help with the construction. The majority of the sediment comes from these tidal flows from the North Sea and English Channel. The lattice Boltzmann method shallow water equations, LABSWE, has been used to produce the tidal currents within the harbour. A dredging of 20m has been undertaken in the Outer Harbour. This dredging had small effect and further measures may be necessary to reduce this amount. We considered adding a small breakwater within the western harbour's entrance and extending the western arm creating a smaller entrance for turbulent flow which is a major contributor to sediment deposit. This had significant impact into the reduction of flow within the harbour and therefore a potential increase into the average run time for the harbour, allowing for the smaller vessels that use this section have less delays overall.

Keywords: Lattice Boltzmann method; shallow water equations; LABSWE; Dover harbour; sediment dredging.

1. Introduction

Dover Harbour, considered to be busiest passenger harbour in Europe, experiences a build-up of silt and sediment predominantly around the two main entrances. Up to $250,000\ m^3$ of mud and sand is deposited away from the harbour however due to the strong tidal currents from both the North Sea and the English Channel these areas fill up quickly. The movement of the tidal flows across the harbour exceeds the threshold shear stress of the bed causing the transport of sediment to these areas (Dey 1999).

Since 2018 a revival of Dover Harbours western dock has been taken place to grant new opportunities and investment into the harbour. This change will expand the western docks and add a new area to house small vessels. The revival will use dredged material to help with the construction of the expanded areas. However once the Dover Western Dock Revival, also known as DWDR, has been completed will this new expansion change tidal flows within the harbour and potentially increase the amount to be dredged. If so can the harbour be dredged further to reduce the turbulent waters that may enter the harbour.

Shallow seas, such as those seen in the Strait of Dover, differ from their larger, deeper counterparts due to the geostrophic acceleration, coastal boundaries, etc. acting upon them (Bowden 1956). These factors influence the tidal currents greatly. Breakwaters have a considerable impact and prevent turbulent erratic flow from entering the harbour and preventing travel. The breakwater around Dover harbour started to be built within 1847 to decrease these influences (Vernon-Harcourt 1885). The water

³³ renovation and flushing from the harbour has been studied by Sanchez-Arcilla (2002) as it has the
³⁴ effect of having two entrances to the harbour.

³⁵ The effect of both the North Sea and the English Channel give a residual circulation pattern that ebbs
³⁶ and flows high and low tides (Prandle et al. 1993). These tides directly affect the harbour by flowing
³⁷ across the top of it thus creating small inner vortices both inside and outside of the harbour. The
³⁸ vortices created by these two differing flows has been observed both in Dover and in Calais (Latteux
³⁹ 1980).

⁴⁰ The lattice Boltzmann method, LBM, has shown promise as a modern numerical method for solving
⁴¹ incompressible flow problems (Guo, Shi, and Wang 2000) and is a successor to the lattice gas automata,
⁴² (Wolf-Gladrow 2000) which comprised of Boolean logic to determine where particles lay within a
⁴³ system. The role of the lattice Boltzmann method is to describe the simulation through the mesoscopic
⁴⁴ range, the bridge between the microscopic and the macroscopic worlds (McNamara and Zanetti
⁴⁵ 1988). In this range a group of particles are considered rather than mapping the complete particle
⁴⁶ interactions. Then the macroscopic quantities are developed and associated to the system, necessary
⁴⁷ for the formulation of the Navier-Stokes equations. This allows the method to be easily paralleled
⁴⁸ (Huang et al. 2015).

⁴⁹ The shallow water equations, SWE, have been used to model a wide range of flow problems from
⁵⁰ tidal flows with a good amount of accuracy (Kelly et al. 2016) to open channel flows (Peng, J. G. Zhou,
⁵¹ and Burrows 2011). Zhou has proposed a conjunction of the nonlinear SWE with the LBM, LABSWE,
⁵² for river and coastal engineering. The LABSWE has been adopted due to its efficiency and simplicity
⁵³ particularly when dealing with boundary conditions (J.G. Zhou 2007).

⁵⁴ Within this paper a look into how the new revival of the Western Harbour within Dover Harbour
⁵⁵ effects the tidal flows using the LABSWE method.

⁵⁶ 2. Methodology

⁵⁷ 2.1. Governing Equations

⁵⁸ The 2D SWE with source terms of bed slope and bed friction may be written in tensor notation as

$$\begin{aligned} \frac{\partial h}{\partial t} + \frac{\partial(hu_i)}{\partial x_i} &= 0, \\ \frac{\partial(hu_i)}{\partial t} + \frac{\partial(hu_i u_j)}{\partial x_j} &= -g \frac{\partial h^2}{\partial x_i} \frac{h^2}{2} - gh \frac{\partial z_b}{\partial x_u} - \frac{\tau_{bi}}{\rho} + \frac{\partial}{\partial x_j}(h\nu \frac{\partial u_i}{\partial x_j}) \end{aligned} \quad (1)$$

⁵⁹ where i, j are the indices and the Einstein summation convention is used therefore if a repeated indices
⁶⁰ is used then a summation over the space coordinates. The Cartesian coordinate is x_i , h is the water
⁶¹ depth, t is the time, u_i is the depth-averaged velocity component in the i direction, z_b is the bed
⁶² elevation, $g = 9.81 \text{ m/s}^2$ is the acceleration due to gravity, ρ is the water density, ν the viscosity, τ_{bi} the
⁶³ bed shear stress along the $i - th$ direction defined by

$$\tau_{bi} = \rho C_b u_i \sqrt{u_j u_j} \quad (2)$$

⁶⁴ where C_b is the bed friction coefficient.

⁶⁵ 2.2. Lattice Boltzmann Model

⁶⁶ The Bhatnagar, Gross Krook Method (1953), also known as the single-relaxation time method, SRT, has
⁶⁷ been modified to calculate the SWE (Zhou 2011)

$$f_i(x + e_i \delta t, t + \delta t) - f_i(x, t) = \frac{1}{\tau} (f_i^{eq} - f_i) + \frac{\delta t}{6e^2} e_{ij} F_j \quad (3)$$

where f_i and f_i^{eq} is the particle distribution function and the particle equilibrium function respectively, x is the two dimensional Cartesian coordinate of space, t is the time unit, δt is the time step, e_i is the particle velocity vector described upon the lattice configuration in Figure 1 where $i = 0, \dots, 8$, e_{ij} is the particle velocity component within the j direction, $e = \delta x / \delta t$ where δx is the lattice size, and τ is the single-relaxation parameter which is related to the depth-averaged eddy viscosity ν by

$$\tau = \frac{6\nu + 1}{2}. \quad (4)$$

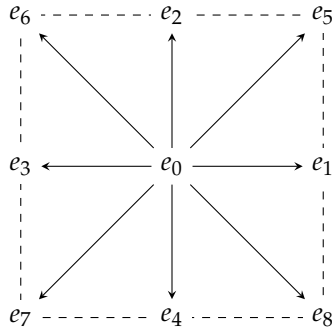


Figure 1. A two-dimensional 9 vertex lattice.

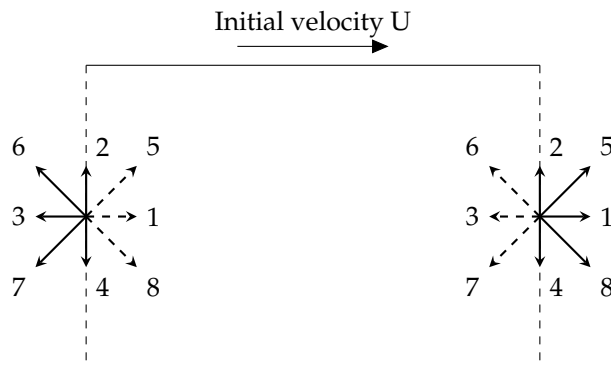


Figure 2. Example of a channel flow describing the boundary conditions

f_i^{eq} is defined as

$$f_i^{eq} = \begin{cases} h(1 - \frac{5gh}{6e^2} - \frac{2u^2}{3e^2}) & \text{if } i = 0, \\ h(\frac{gh}{6e^2} + \frac{e_i u}{3e^2} + \frac{e_i^2 u^2}{2e^4} - \frac{u^2}{6e^2}) & \text{if } i = 1, 2, 3, 4, \\ \frac{1}{4}h(\frac{gh}{6e^2} + \frac{e_i u}{3e^2} + \frac{e_i^2 u^2}{2e^4} - \frac{u^2}{6e^2}) & \text{if } i = 5, 6, 7, 8. \end{cases} \quad (5)$$

The forcing term F_i is given by

$$F_i = -gh \frac{\partial z_b}{\partial x_i} + \frac{\tau_{wi}}{\rho} - \frac{\tau_{bi}}{\rho} + \Omega h u_y \delta_{ix} - \Omega h u_x \delta_{iy}, \quad (6)$$

where h and u_i is the average water depth and the depth-averaged velocity, $g = 9.81 m/s^2$ is the acceleration due to gravity, z_b is the bed elevation, τ_{wi} is the wind shear stress, τ_{bi} is the bed shear

⁷⁷ stress, ρ is the water density, Ω is the Coriolis parameter to take the Earth's rotation into effect, and δ_{ij}
⁷⁸ is the Kronecker delta function given by

$$\delta_{ij} \begin{cases} 0, & \text{if } i = j, \\ 1, & \text{if } i \neq j. \end{cases} \quad (7)$$

⁷⁹ The macroscopic variables of both water depth and velocity are

$$h = \sum_{i=0}^8 f_i, \quad (8)$$

$$u = \frac{1}{h} \sum_{i=0}^8 e_i f_i \quad (9)$$

⁸⁰ 2.3. Boundary Conditions

⁸¹ For the current simulations a combination of both non-slip and Zou-He boundary conditions have
⁸² been implemented. For the non-slip, also known as a traditional bounce-back boundary condition, the
⁸³ particle is reflected from a solid surface. These conditions have been used at the solid boundaries of
⁸⁴ the harbour and across the south, east and west boundaries of the cavity as seen in Figure 2. The LBM
⁸⁵ solves these conditions through

$$\begin{aligned} f_1 &= f_3, & f_2 &= f_4, \\ f_5 &= f_7, & f_6 &= f_8. \end{aligned} \quad (10)$$

⁸⁶ A non-slip boundary condition has also been applied to the challenging harbour geometry. For this
⁸⁷ complicated geometry the last known fluid node available before colliding with the curved boundary
⁸⁸ is used and the next known area after the collision is represented as a solid. Figure 3 represents this
⁸⁹ technique.

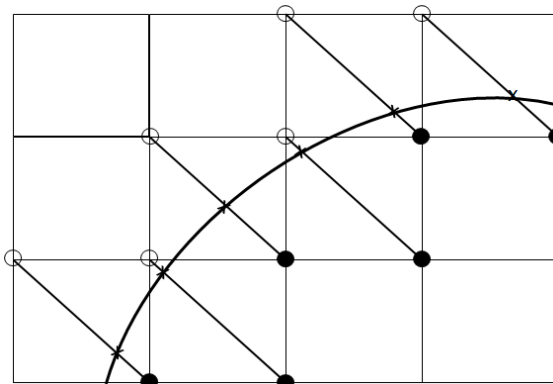


Figure 3. Layout of a regularly spaced lattice with a curved boundary. The thick curve represents the curved boundaries location. The x upon the boundary curve represents the particle collision boundary. The empty and shaded circles denote the fluid and solid nodes respectively.

⁹⁰ Using the boundary conditions posed by Liu et.al. (2012) both the inlet and outlet boundary conditions
⁹¹ can be discovered. They proposed that the boundary conditions can be found using a mass and
⁹² momentum balance following the Zou-He boundary conditions (Zou and He 1997). Take the inlet on
⁹³ the left-handside for example, the unknown velocity vectors, e_1, e_5 and e_8 , can be extrapolated using the
⁹⁴ known vectors. Hence discovering



Figure 4. Topological map of Dover Harbour

$$\begin{aligned} f_1 &= f_3 + \frac{2hu}{3e}, \\ f_5 &= \frac{hu}{6e} + f_7 + \frac{f_4 - f_2}{2}, \\ f_8 &= \frac{hu}{6e} + f_6 + \frac{f_2 - f_4}{2}. \end{aligned} \quad (11)$$

95 However this scheme does not fully close as both the velocity and water-depth are unknown at the
 96 inlet. Two new steps that conserve both the mass and momentum of the system, these two steps are the
 97 assigning and compensation step respectively. For the assigning step a zero-gradient boundary is used
 98 at the inlet for the macroscopic variables, h, u and v . For the compensation step the discharge per
 99 unit width, hu , is converted to $(Q_{in} - Q_c)/b$. Where Q_{in} is the constant discharge, Q_c is the discharge
 100 calculated within the assigning step using h, u and v , and b is the width of the channel. Thus the new
 101 inlet boundary conditions can be defined as

$$\begin{aligned} f_1 &= f_3 + \frac{2hu}{3e}, \\ f_5 &= \frac{hu + (Q_{in} - Q_c)/b}{6e} + f_7 + \frac{f_4 - f_2}{2} + \frac{hv}{2e}, \\ f_8 &= \frac{hu + (Q_{in} - Q_c)/b}{6e} + f_6 + \frac{f_2 - f_4}{2} - \frac{hv}{2e}. \end{aligned} \quad (12)$$

102 3. Results

103 A 400x400 domain was created to represent the Dover Harbour space seen on the right hand side of
 104 Figure ?? with an initial velocity at the inlet upon the left hand-side set to $u = 1m/s^2$. The simulations
 105 water depth was set to $h = 6m$ to represent the high water, HW, tides seen within Dover. The discharge
 106 rate was set to $Q = 2.2m/s^3$.

107 Using satellite imagery areas of the harbour were analysed and drawn to represent the more
 108 complicated geometry of the harbour. Then using the topological data found in 4 the bed elevation
 109 can be found for a more accurate representation of the tidal flows. Using this map an approximation
 110 of the shallow and deep waters can be obtained. For simplicity the green areas are estimated to be
 111 of a higher elevation than the water depth. However using the the mean tidal profile within ?? and
 112 agreement of average depth 0.1m has been established.

113 The average water height has been reduced by about 1:10 to stay within the required SWE stability
 114 range. The time step = 0.01 and ran until the time step was after a 3 hour HW approximation.
 115 These simulations have all been shown at HW as this was the most turbulent time for the harbour in
 116 particular.

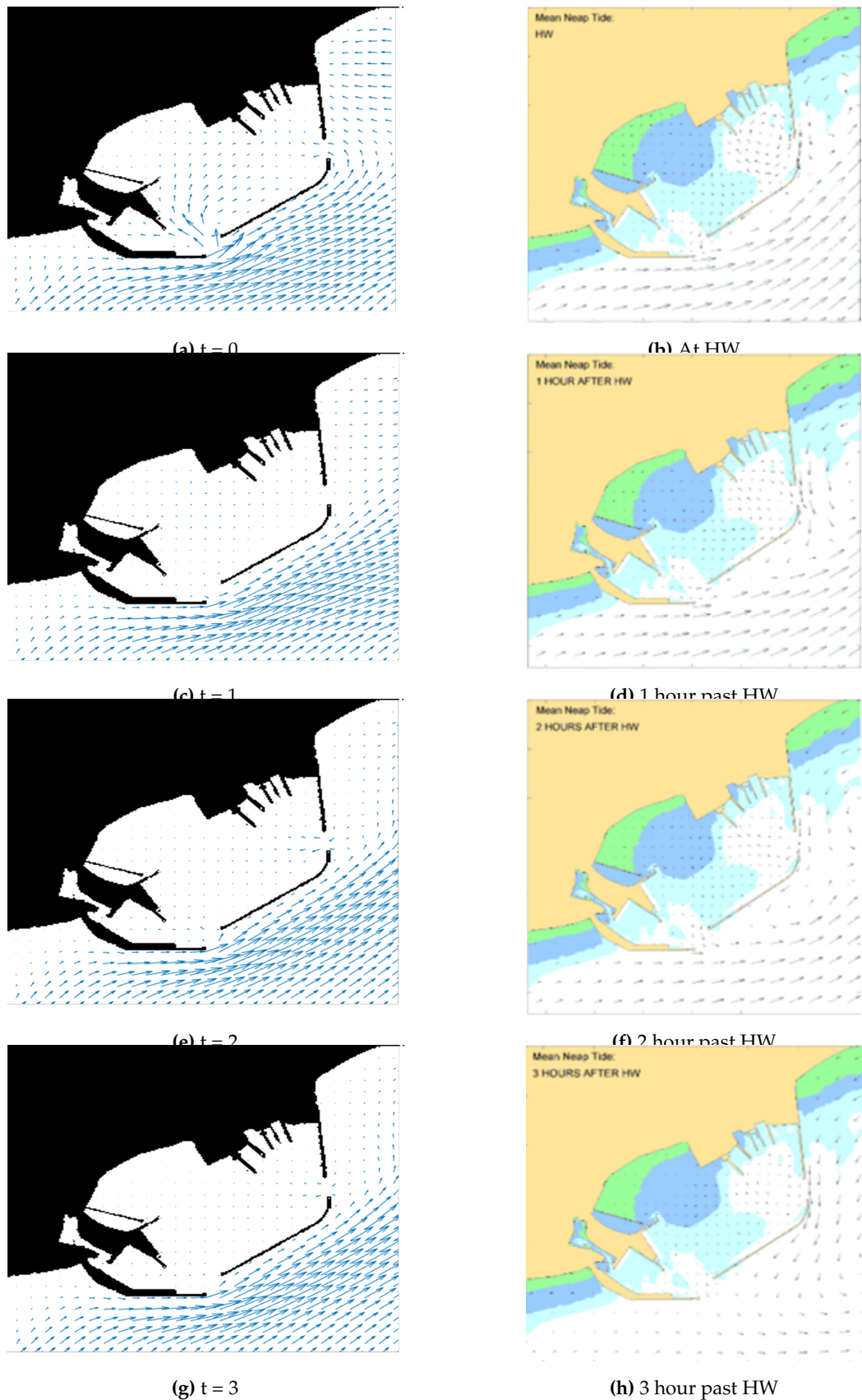


Figure 5. The velocity vector profile of the mean tidal (L) at HW compared with results from HR Wallingford (R) (Masters 2019)

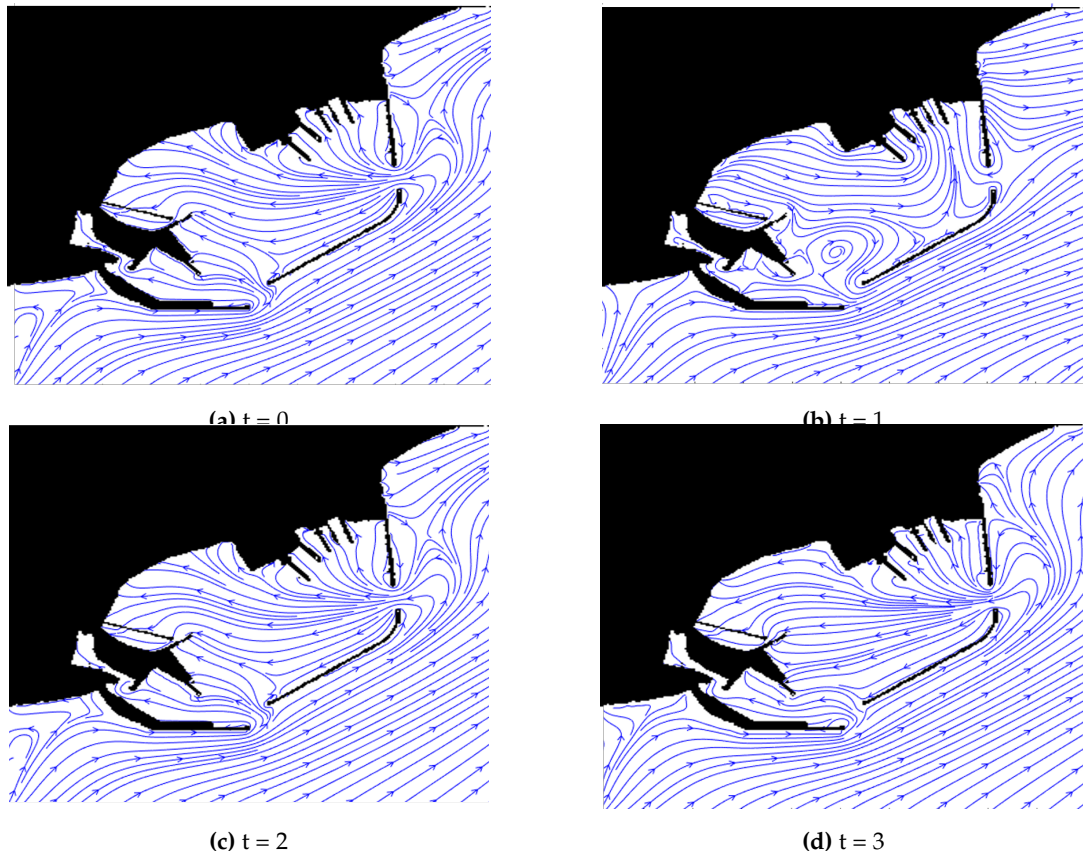


Figure 6. The mean tidal average using the lattice Boltzmann method at HW and three more consecutive hours after HW

117 For the simulation seen within Figures 6 the harbour is using the topological data and the high water
 118 data. When compared to the set seen within Figure 5 many similarities become apparent. A vortex
 119 is being created outside of the harbour due to the breakwater. The outer harbour and the entrances
 120 experience a dramatic decrease in speed compared to the rest of the simulation. Small vortices are seen
 121 to be created within the southern entrance which is where the majority of the smaller vessels depart
 122 from. However within the simulation the large vortex seen within the northern entrance in 5 at both
 123 HW and an hour past does not seem to form within the LBM models. This method has dampened
 124 some of the features seen within the HR Wallingford model as within Figure 5b a vortex can be seen
 125 within the eastern harbour entrance which does not seem to be as prominent within Figure 6a.

126 One key area that is affected predominantly at high tides is the southern entrance. This is created by
 127 the English Channel bypassing the entrance creating vortexes at the entrance. The dredging at the
 128 entrances, seems to affect these the most. Seen within Figures ?? the southern entrance seems to create
 129 more vortices however are much more condensed compared to Figures 6. This can be seen when
 130 looking at the velocity vectors for the two cases, there seems to be more activity at the HW, Figure 7,
 131 than the LW 5.

132 In Figures ?? the bed in the outer harbour has been decreased by 2m along the entrances and near
 133 the breakwater creating a small channel. This has seemed to dampen the more intense vortices being
 134 created within the harbour, primarily within Figure 6b to a more manageable size seen within Figure
 135 7d. Also from this dredged channel more flow seemed to be diverted away from the inner harbour
 136 making it calmer for both vessels and swimmers. When looking at the figures seen within Figure 7 the
 137 slowest speeds are within the inner harbour where the depth is the lowest.

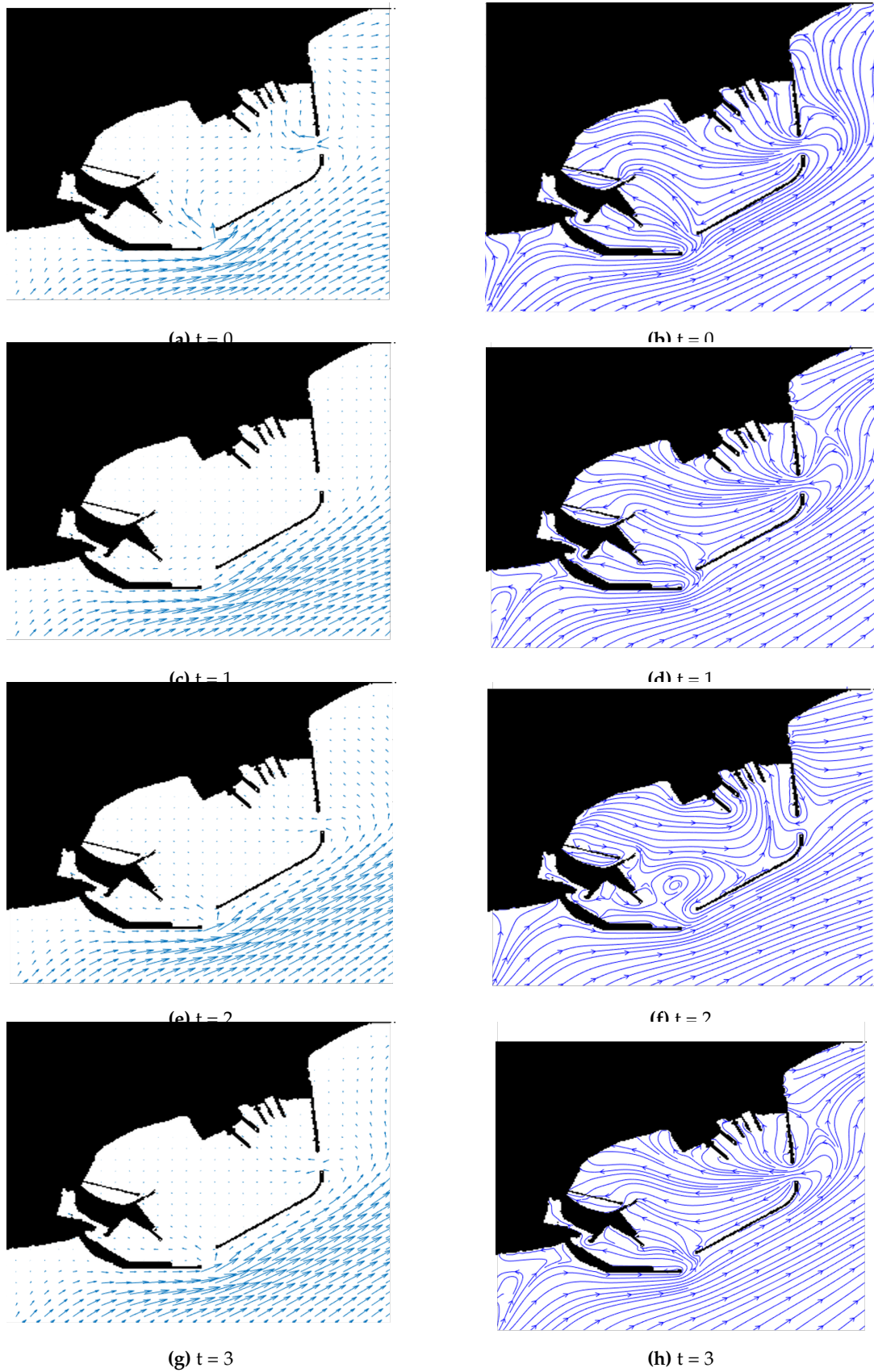


Figure 7. Mean tidal flow velocity vector (L) and the streamline (R) after being dredged by 20m

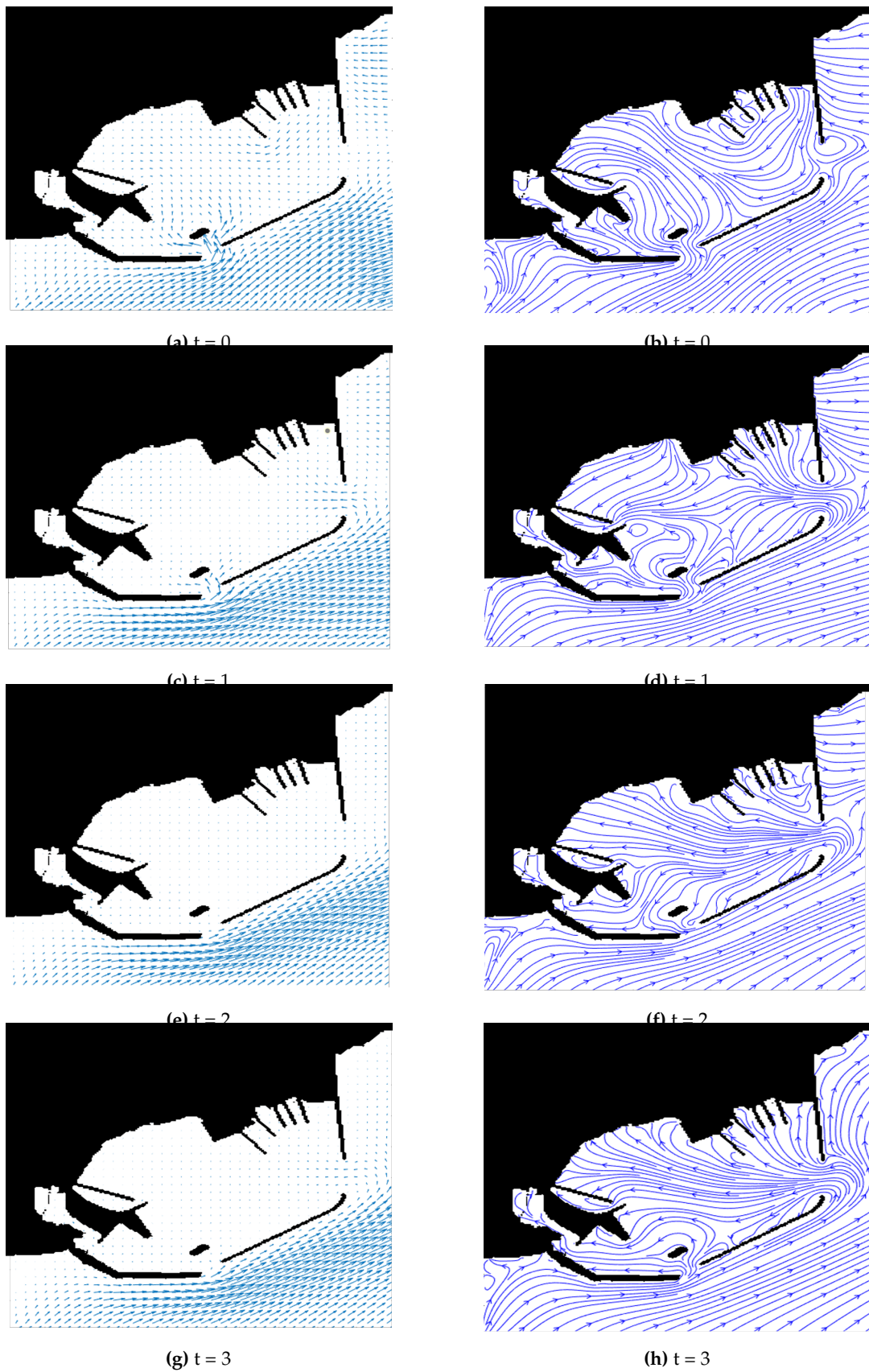


Figure 8. The mean tidal with an extended western harbour breakwater at the opening and a further breakwater within the Outer Harbour area of the western entrance

¹³⁸ Another breakwater was added into the entrance of the western harbour entrance towards the bottom
¹³⁹ of the harbour within the simulations. This was to further reduce the amount of the turbulent flow
¹⁴⁰ entering from this entrance and therefore reduce the amount of sediment that could be transported with
¹⁴¹ those flows. In conjunction with this a small extension was added to the western harbour entrances
¹⁴² breakwater reducing the size of the entrance. As mostly smaller vessels use this entrance a way of
¹⁴³ limiting the amount of tumultuous waters that could effect travel.

¹⁴⁴ Observing the streamlines seen within Figure 8 by extending the breakwater a significant amount of
¹⁴⁵ the flow that comes from the English Channel seen at the left hand bottom portion of the simulation
¹⁴⁶ bypasses the harbour. The breakwater within the Outer Harbour portion of the entrance has a
¹⁴⁷ significant impact upon limiting the amount of flow entering the harbour assuming for safer and easier
¹⁴⁸ travel to and from the new DWDR. However a turbulent vortex is created at when $t = 2$ in Figure 8f
¹⁴⁹ outside of the harbour. This dissipates at the later hours but could be a cause for concern for depositing
¹⁵⁰ sediment outside the harbour affecting travel.

¹⁵¹ 4. Conclusions

¹⁵² The tidal flows seen within Dover Harbour have been modelled using the lattice Boltzmann method.
¹⁵³ Dredging within the harbour looks to be a short term solution at improving the overall flow within
¹⁵⁴ the harbour making it more accessible for vessels to travel particularly around the harbour entrances.
¹⁵⁵ However adding or extending the western harbour entrance with further breakwaters seems to have
¹⁵⁶ significant impact upon the amount of turbulent flow at HW entering the harbour which could limit
¹⁵⁷ the amount of deposited silt and sediment entering the harbour. Therefore a reduction in the amount
¹⁵⁸ needing to be dredged annually.

¹⁵⁹ **Funding:** This research received no external funding

¹⁶⁰ **Conflicts of Interest:** The authors declare no conflict of interest.

¹⁶¹ Abbreviations

¹⁶² The following abbreviations are used in this manuscript:

¹⁶³	LABSWE	Lattice Boltzmann Shallow Water Equation
	DWDR	Dover Western Dock Revival
¹⁶⁴	HW	High Water
	LW	Low Water

¹⁶⁵ References

- ¹⁶⁶ Bhatnagar, P. L., E.P. Gross, and M. Krook (1953). *A Kinetic Approach to Collision Processes in Gases: Small Amplitude Processes in Charged and Neutral One Component Systems*. Tech. rep. Massachusetts:
¹⁶⁷ Massachusetts Institute of Technology.
- ¹⁶⁸ Bowden, K. F. (Feb. 1956). "The Flow of Water through the Straits of Dover, Related to Wind and
¹⁶⁹ Differences in Sea Level". In: *Philosophical Transactions of the Royal Society A: Mathematical, Physical
and Engineering Sciences* 248.953, pp. 517–551. ISSN: 1364-503X. DOI: [10.1098/rsta.1956.0008](https://doi.org/10.1098/rsta.1956.0008).
- ¹⁷⁰ Dey, Subhasish (1999). "Sediment threshold". In: *Applied Mathematical Modelling*. ISSN: 0307904X. DOI:
¹⁷¹ [10.1016/S0307-904X\(98\)10081-1](https://doi.org/10.1016/S0307-904X(98)10081-1).
- ¹⁷² Guo, Zhaoli, Baochang Shi, and Nengchao Wang (2000). "Lattice BGK Model for Incompressible
¹⁷³ Navier-Stokes Equation". In: *Article in Journal of Computational Physics* 165, pp. 288–306. DOI:
¹⁷⁴ [10.1006/jcph.2000.6616](https://doi.org/10.1006/jcph.2000.6616).

- 177 Huang, Changsheng et al. (2015). "Multi-GPU based lattice boltzmann method for hemodynamic
178 simulation in patient-specific cerebral aneurysm". In: *Communications in Computational Physics*.
179 ISSN: 19917120. DOI: [10.4208/cicp.2014.m342](https://doi.org/10.4208/cicp.2014.m342).
- 180 Kelly, Samuel M et al. (2016). "A Coupled-Mode Shallow-Water Model for Tidal Analysis: Internal Tide
181 Reflection and Refraction by the Gulf Stream". In: *JOURNAL OF PHYSICAL OCEANOGRAPHY*
182 46, pp. 3661–3679. DOI: [10.1175/JPO-D-16-0018.1](https://doi.org/10.1175/JPO-D-16-0018.1).
- 183 Latteux, B. (1980). "Harbour Design Including Sedimentological Problems Using Mainly Numerical
184 Techniques". In: *Coastal Engineering*.
- 185 Liu, H., J.G. Zhou, and R. Burrows (2012). "Inlet and outlet boundary conditions for the
186 Lattice-Boltzmann modelling of shallow water flows". In: *Progress in Computational Fluid Dynamics,
187 An International Journal*. ISSN: 20500416. DOI: [10.1002/jib.143](https://doi.org/10.1002/jib.143).
- 188 Masters, Steve. (2019). *Mean Spring Tide Tidal Currents*. Tech. rep. Dover: Port of Dover, p. 5.
- 189 McNamara, Guy R. and Gianluigi Zanetti (Nov. 1988). "Use of the Boltzmann Equation to Simulate
190 Lattice-Gas Automata". In: *Physical Review Letters* 61.20, pp. 2332–2335. ISSN: 0031-9007. DOI:
191 [10.1103/PhysRevLett.61.2332](https://doi.org/10.1103/PhysRevLett.61.2332). URL: <https://link.aps.org/doi/10.1103/PhysRevLett.61.2332>.
- 192 Peng, Y, J G Zhou, and R Burrows (2011). "Modelling solute transport in shallow water with the lattice
193 Boltzmann method". In: DOI: [10.1016/j.compfluid.2011.07.008](https://doi.org/10.1016/j.compfluid.2011.07.008).
- 194 Prandle, D. et al. (June 1993). "The influence of horizontal circulation on the supply and distribution of
195 tracers". In: *Philosophical Transactions of the Royal Society of London. Series A: Physical and Engineering
196 Sciences* 343.1669, pp. 405–421. DOI: [10.1098/rsta.1993.0055](https://doi.org/10.1098/rsta.1993.0055).
- 197 Sanchez-Arcilla, A. et al. (2002). "Water Renovation in Harbour Domains. The Role of Wave and Wind
198 Conditions". In: *Coastal Engineering 2002*. WORLD SCIENTIFIC. ISBN: 978-981-238-238-2.
- 199 Vernon-Harcourt, L.F. (1885). *Harbours and Docks*. Cambridge: Cambridge University Press, p. 650.
200 ISBN: 978-1-108-07202-1.
- 201 Wolf-Gladrow, Dieter A. (2000). *Lattice Gas Cellular Automata and Lattice Boltzmann Models*. ISBN:
202 978-3-540-66973-9. DOI: [10.1007/b72010](https://doi.org/10.1007/b72010).
- 203 Zhou, J (2011). "Enhancement of the LABSWE for shallow water flows". In: *Journal of Computational
204 Physics*. DOI: [10.1016/j.jcp.2010.09.027](https://doi.org/10.1016/j.jcp.2010.09.027).
- 205 Zhou, J.G. (2007). "Comparison study of lattice Boltzmann method and Godunov method for shallow
206 water flows". In: *Proceedings of 32nd Congress of IAHR*, Venice.
- 207 Zou, Qisu and Xiaoyi He (1997). "On pressure and velocity flow boundary conditions and bounceback
208 for the lattice Boltzmann BGK model". In: *Physics of Fluids* 9.6, pp. 1591–1598. DOI: [10.1063/1.869307](https://doi.org/10.1063/1.869307).

210 © 2020 by the authors. Submitted to *Journal Not Specified* for possible open access
211 publication under the terms and conditions of the Creative Commons Attribution (CC BY) license
212 (<http://creativecommons.org/licenses/by/4.0/>).